ZOOM-DEPENDENT CAMERA CALIBRATION

Salaheddin Al-Ajlouni, PhD student
Clive Fraser, Professor
Department of Geomatics
The University of Melbourne
Victoria 3010, Australia
sajlouni@sunrise.sli.unimelb.edu.au
c.fraser@unimelb.edu.au

ABSTRACT

The application of consumer-grade digital cameras for photogrammetric measurement is subject to the requirement that imagery is recorded at pre-set or fixed zoom and focus settings. The camera is then metrically calibrated or self-calibrated for the lens setting employed. This requirement arises because camera calibration parameters, and especially those related to lens distortion, vary significantly with the zoom/focus setting. In this presentation, a zoom-dependent calibration process is proposed whereby the traditional image coordinate correction model for camera interior orientation and lens distortion is expressed as a function of the nominal zoom focal length written to the EXIF header of the image file. This removes the requirement to utilize fixed zoom/focus settings for the images forming the photogrammetric network. A review of the behavior of camera calibration parameters with varying zoom setting is first presented, after which the newly developed zoom-dependent calibration model will be described. Experimental results from its application to a number of 'off-the-shelf' cameras are then analyzed. These demonstrate that the proposed approach is suitable for numerous applications of medium-accuracy digital close-range photogrammetry, across fields as diverse as traffic accident reconstruction and heritage recording.

INTRODUCTION

One of the main constraints applying to the adoption of off-the-shelf cameras is the requirement to record images or subsets of images at fixed focus and/or zoom settings. This requirement arises because camera calibration parameters, especially those related to lens distortion, vary significantly with changing focal length (Fraser, 1997; Brown, 1971). The user of digital close range photogrammetry may record images with different focus or zoom settings. However, in such cases either metric calibration is required for all lens settings employed, or in the case of self-calibration, the sub-networks formed by multiple images at particular focal length values must display a geometry that will support recovery of the parameters of interior orientation and lens distortion. Brown (1971) formulated a model for the variation of radial distortion with changing focus, which has been applied in high-accuracy industrial photogrammetry. Moreover, this model can be used as a constraint in the self-calibration of cameras at multiple focal settings (Fraser, 1980).

In the context of consumer grade cameras, however, models describing variation of lens distortion with changing focus are generally of limited utility for the short focal length integrated zoom lenses because the variation of radial distortion is likely to diminish to a negligible level at focused distances beyond 15 focal lengths (Fryer & Brown, 1986; Fraser & Shortis, 1990). Most consumer grade digital cameras have a maximum zoom focal length of around 30mm. Hence, for all practical purposes images recorded by these cameras for photogrammetric application can be considered infinity focused. The same situation does not apply to variations in zoom setting, where principal distance and lens distortion vary significantly as the lens is zoomed in or out. This can be a problem in off-the-shelf cameras, which invariably have zoom lenses but not necessarily mechanisms to re-set a given focal length.

In order to address the problem of supplying calibration parameters for a consumer grade camera with an integrated zoom lens, the Zoom-Dependent (Z-D) calibration method has been developed. In this approach, the image coordinate correction models can be expressed as a function of lens focal length throughout the full zoom range. The method requires first that the nominal focal length is written to the EXIF header (Exchange Image Format) for each captured image, and secondly that the camera has been initially self-calibrated at three zoom settings, nominally zoomed fully in, out and at the mid range. The Z-D calibration model is intended for use in medium accuracy applications such as traffic accident reconstruction, process plant documentation and cultural heritage recording, where a proportional accuracy level in object space positioning of 1: 5,000 or lower is the norm.

In the following sections a general review of camera calibration with changing zoom settings is presented. The development of the Z-D calibration process is then described. Finally, experimental results for four digital cameras are analyzed in terms of the impact of Z-D calibration upon metric accuracy. The present paper is a condensed version of Al-Ajlouni & Fraser (2006).

VARIATION IN CALIBRATION WITH ZOOM SETTING

Principal Distance

Since the Z-D calibration parameters are determined as a function of the recorded nominal focal length written to the EXIF header, it is necessary to build a relationship between the recorded focal length (f) and the photogrammetric principal distance (c). Shown in Table 1 are the differences between f and c for four cameras: a Canon PowerShot S30 and G1, Canon IXUS V and a Nikon D100 SLR-type camera with an external 24-85mm zoom lens. It is apparent that the differences are not constant and not linear. But since the Z-D calibration process requires full self-calibration at three different zoom settings, here the user has a few options for modeling the variation of principal distance. These include the assumption that the discrepancy between f and c is constant, or that the variation is linear, or can be modelled by a first-order polynomial. For the applications described in this paper, a linear variation function has been adopted for the determination of c from f.

Table 1. Differences between principal distance (c) and focal length (f) for multiple zoom settings; units are mm

Canon PowerShot S30		Canon PowerShot G1		Canon IXUS V		Nikon D100 with 24-85mm lens	
Zoom Setting	Difference c-f	Zoom Setting	Difference c-f	Zoom Setting	Difference c-f	Zoom Setting	Difference c-f
7.1	0.42	7	0.27	5.4	0.12	24	1.7
8.6	0.35	10.8	-0.10	6.7	-0.06	35	0.8
10.3	0.31	16.8	0.05	8.0	-0.12	50	0.8
12.3	0.32	18.8	0.24	9.3	-0.14	70	2.2
17.5	0.26	21.0	-0.07	10.8	-0.37	85	0.4
21.3	-0.30						

Principal Point Offset

Shown in Fig. 1 are the principal point coordinate values at multiple zoom settings for the four cameras referred to earlier. Also plotted in the figure are the best-fit linear variation functions computed from the three zoom settings indicated by the solid dots for each camera. It can be seen that some of the cameras show near linear variation, which suggests near constant alignment of the optical axis with the focal plane. But others display a non-linear variation behaviour, as previously observed by Burner (1995), Wiley & Wong (1995) and Noma et al. (2002).

Given the fact that there is a high projective coupling between the decentering distortion and the principal point offsets, it is quite difficult to fully isolate the two set of parameters from each other. One has little option here other than to consider the variation of principal point offsets with changing zoom setting to be linear. Thus, a linear model has been adopted for the Z-D calibration.
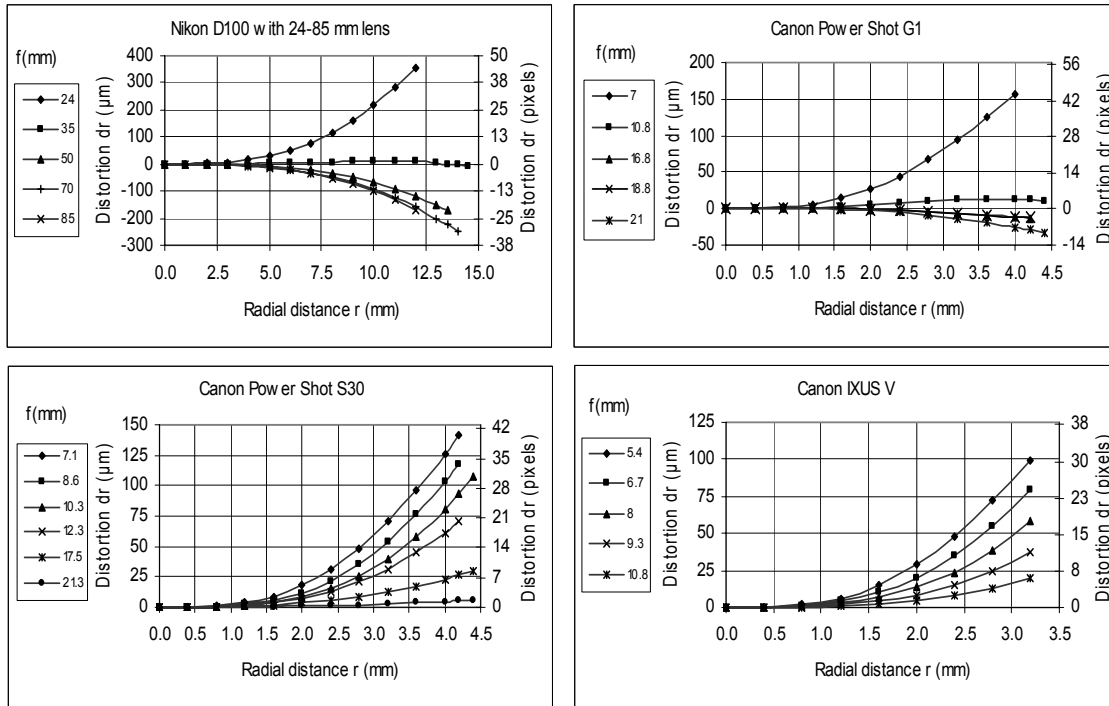
Radial Lens Distortion

The variation of radial lens distortion with changing focus tends to be negligible for consumer-grade cameras and is also typically ignored in other than very high accuracy close-range photogrammetry applications. The contrary is true when it comes to the variation of radial distortion with changing zoom setting. Fig. 2 shows the Gaussian radial lens distortion profiles at different zoom settings for the 2-megapixel IXUS V, 3-megapixel PowerShot S30 and G1, and the 6-megapixel Nikon D100 with 24-85mm zoom lens. Radial distortion is modelled here by the well-known formula

$$dr = K_1 r^3 + K_2 r^5 + K_3 r^7 \qquad (1)$$

where dr is the radial lens distortion, K_i the coefficients of radial distortions and r the radial distance. These profiles are plotted to the maximum encountered radial distance in the self-calibration surveys conducted, ie extrapolated values to the corner of the image format are not shown.
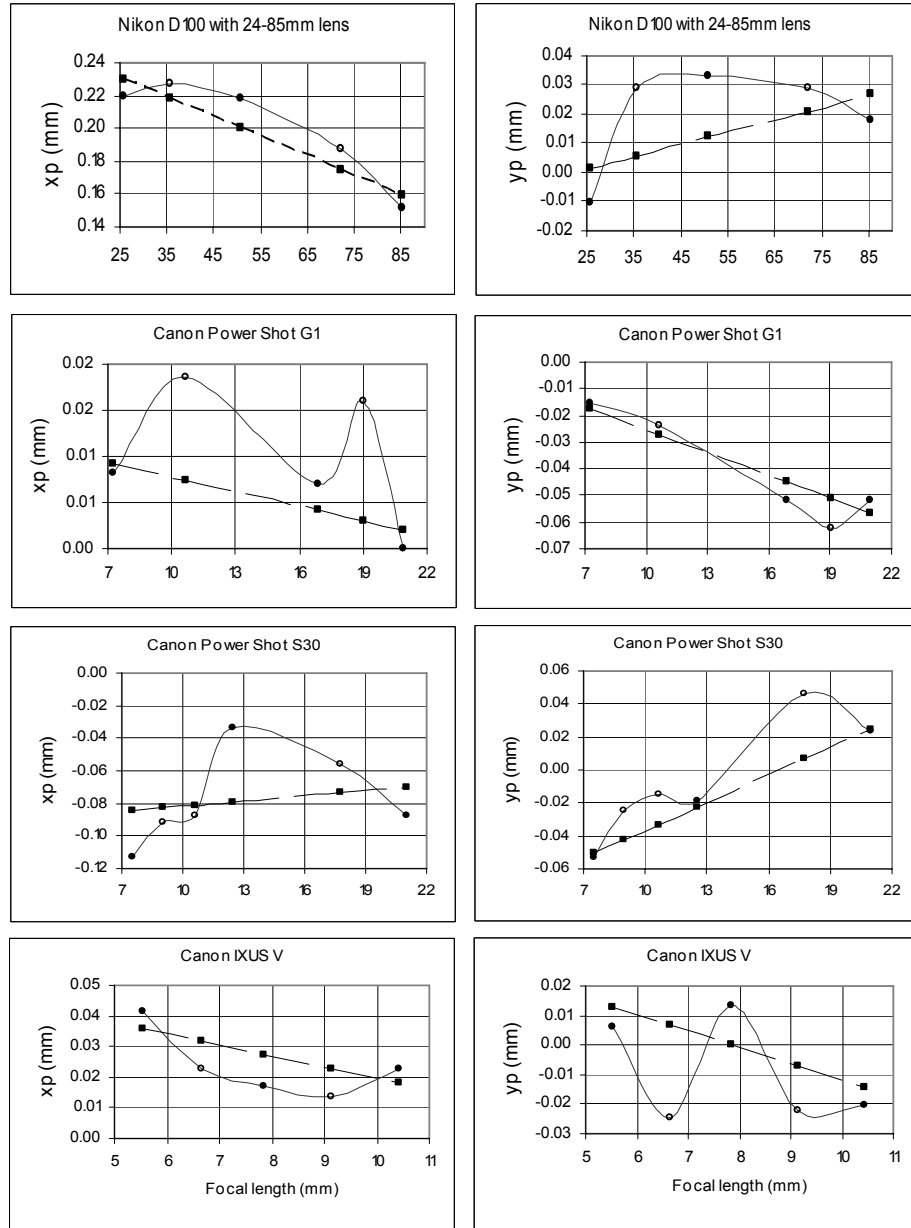
Figure 1. Variation of principal point coordinates x_p and y_p with varying zoom setting (solid line) and best-fit linear variation function (dashed line) determined from three zoom settings (solid dots).

Figure 2. Variation of Gaussian radial distortion with zoom setting.

Noteworthy from Fig. 2 are, firstly, that the variation of radial lens distortion is non linear; secondly, that the maximum radial distortion occurs at the minimum focal length, even in cases of a zero crossing; thirdly, that the cubic term of radial distortion K_1 decreases monotonically with increasing focal length; and, finally, that these profiles are almost cubic, which reflects the very small contribution to radial lens distortion from the K_2 and K_3 terms. These characteristics should be familiar to photogrammetrists who have employed amateur cameras (eg Laebe & Foerstner, 2004; Wiley & Wong, 1995; Burner, 1995; Fryer, 1986).

Under the assumption that the fifth- and seventh-order terms do not contribute significantly to the radial distortion profile, K_2 and K_3 can be suppressed from Eq.1. The modeling of variation in radial lens distortion with changing zoom settings needs then to consider only the behaviour of K_1. Plots of the variation of K_1 with zoom setting for the four subject cameras are shown in Fig. 3. After an empirical investigation, the optimal model describing the variation in the cubic lens distortion coefficient was found to be

$$K_1^{(c_i)} = d_0 + d_1 c_i^{d_2} \tag{2}$$

where c_i is the principal distance. In the present case the power of the curve indicated by the coefficient d_2 ranged from -0.2 to -3.1. Plots of the variation functions computed for the four cameras are also illustrated in Fig. 3.

Decentering Distortion

Decentering distortion varies with changing zoom settings (eg Fryer & Brown, 1986; Wiley & Wong, 1995). However, there are no reported attempts to model this variation, principally because decentering distortion itself is generally quite small, its significance appearing only in high accuracy photogrammetric applications. Moreover, a significant component of the decentering distortion can be absorbed in the self-calibration process by the principal point coordinates x_p and y_p, especially at longer focal lengths. Shown in Fig. 4 are the decentering distortion profiles at different zoom settings for the four cameras. These profiles are obtained via the following formula (Brown, 1966):

$$P(r) = (P_1^2 + P_2^2)^{1/2} r^2 \tag{3}$$

It can be seen from Fig. 4 that the decentering distortion profile values are less than one pixel, except at the outer edge of the image format. Experiments have showed that the omission of decentering distortion in close-range

photogrammetry utilising off-the-shelf cameras has no practical impact upon the final accuracy of 3D object point coordinates. Because of this, decentering distortion will not be considered further in the Z-D calibration process.
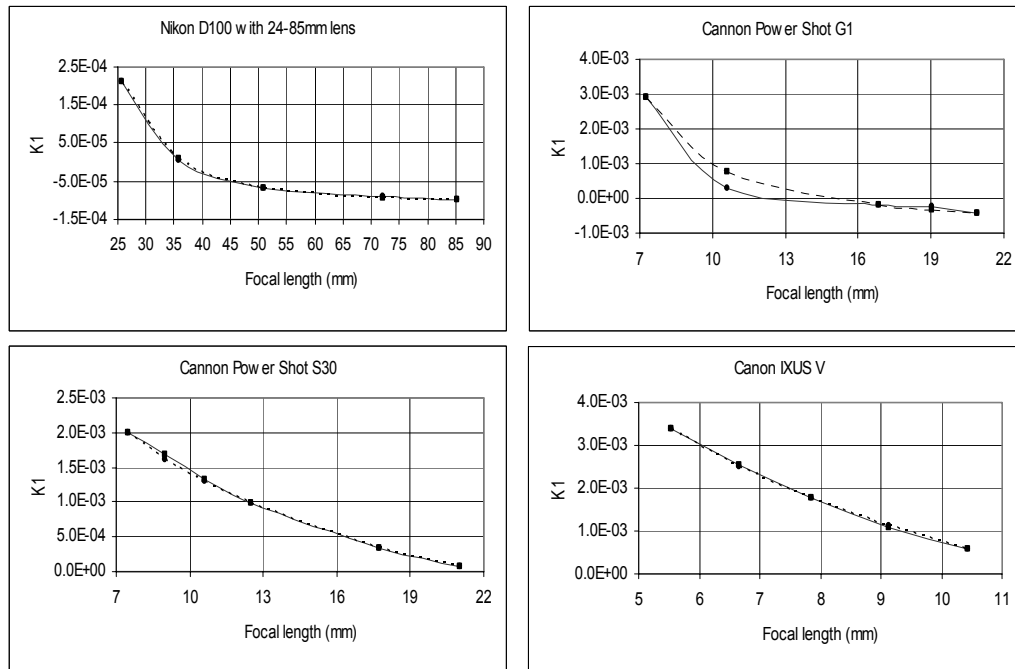

Figure 3. Variation of K_1 with changing zoom setting (solid line) and variation function for $K_1^{(ci)}$ (dashed line).
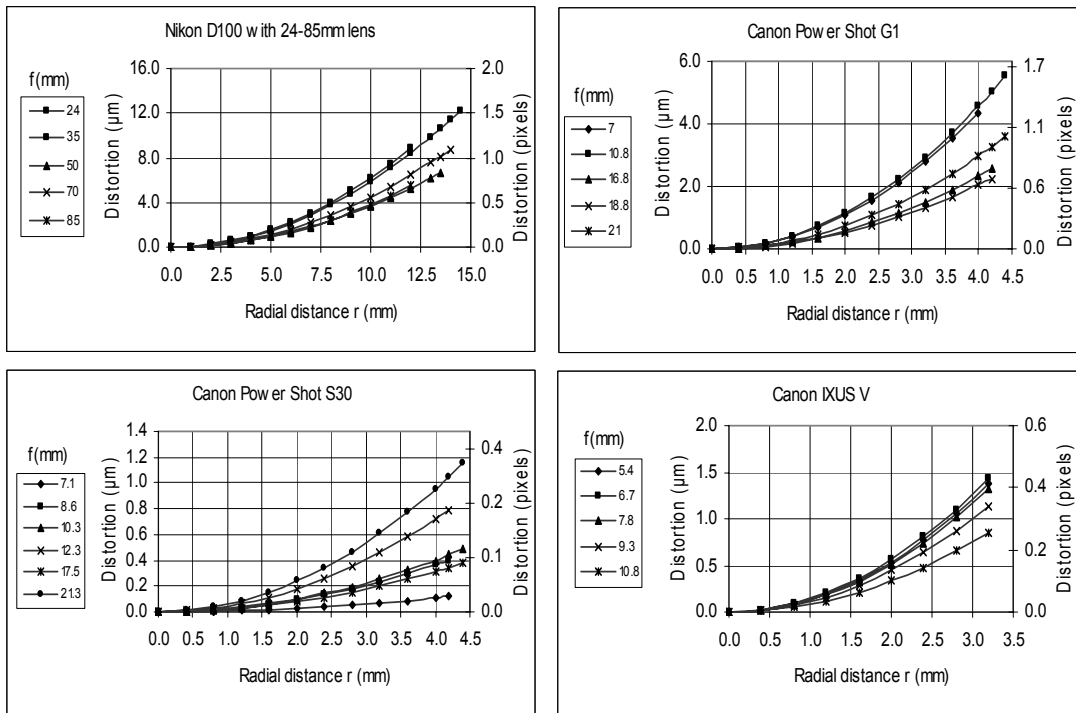

Figure 4. Variation of decentering distortion profile $P(r)$ with changing zoom setting.

DEVELOPMENT OF Z-D CALIBRATION METHOD

The proposed Z-D calibration model associated with the image coordinates correction function is given as

$$x^{corr} = x - x_p^{(c_i)} + \left(x - x_p^{(c_i)}\right)K_1^{(c_i)}r^2$$
$$y^{corr} = y - y_p^{(c_i)} + \left(y - y_p^{(c_i)}\right)K_1^{(c_i)}r^2$$

(4)

where x and y are the measured image coordinates, x^{corr} and y^{corr} the corrected image coordinates, and r the radial distance given by $r = \left(\left(x - x_p^{(c_i)}\right)^2 + \left(y - y_p^{(c_i)}\right)^2\right)^{0.5}$. The individual Z-D calibration parameters are obtained as follows:

Principal distance: $\qquad\qquad c_i = a_0 + a_1 f_i$ (5)

Principal point coordinates: $\quad x_p^{(c_i)} = b_0 + b_1 x_{p_i}$ (6)
$$y_p^{(c_i)} = b_2 + b_3 y_{p_i}$$

Cubic term of radial lens distortion $K_1^{(c_i)}$: as per Eq.(2)

The parameters a_i, b_i of the linear variation functions in Eqs. 5 and 6 can be solved from two full self-calibrations, preferably at the hard limits of the zoom range. A further initial self-calibration, preferably at mid-zoom setting, is needed for the determination of $K_1^{(c_i)}$. However, nothing prevents the user from performing additional self-calibrations to improve the precision of the empirical model.

The Z-D calibration model has the potential of freeing the user from the requirement of recording images, or a sub set of images, at fixed focus and/or zoom setting. Provided that the focal length is written to the EXIF header for each image, the calibration parameters can be empirically modelled for the focal length associated with that image.

EXPERIMENTAL EVALUATION

In order to assess the validity of the Z-D calibration method for consumer grade cameras, a series of experiments was performed with the four cameras already referred to, at different zoom settings. The accuracy of the 3D object point coordinates obtained by the Z-D calibration method was then evaluated against that obtained via the standard self-calibration approach.

Test Field

A targeted 5m x 3m test field consisting of 140 well distributed retro-reflective targets was constructed. All object points had been previously measured, again photogrammetrically, to a 3D positional accuracy (RMS 1-sigma) of 0.04mm. The target array and adopted network geometry for each zoom setting, for each camera, are shown in Fig. 5. The convergent network consisted of six camera stations, at each of which two images were recorded, one being rolled 90°. In addition, two stations were added for evaluation of the Z-D calibration in the case of a stereo image pair. Due to the range of zoom focal lengths involved, from 5.5mm to 85mm, all points were not imaged in all networks. The resulting accuracy will thus be presented in scale-independent form as well as in absolute units because of the different image scales involved.

Determination of Z-D Calibration Parameters

For the D100, Canon IXUS and PowerShot G1, networks were recorded at five zoom settings, whereas six focal length settings were adopted for the Canon PowerShot S30. All image coordinates were measured automatically using the *Australis* software system (Fraser & Edmundson, 2000; Photometrix, 2006). Even though the Z-D calibration method is not intended for high accuracy applications, every effort was made to optimize measurement accuracy, so that 3D positioning discrepancies could be more fully attributed to the distinction between standard self-calibration and the Z-D calibration approach, which involved an empirical modeling of the camera calibration parameters. The computational procedure adopted for the evaluation of each camera was as follows:

    a) A self-calibration was initially performed for each network, in which the additional parameters (APs) of c, x_p, y_p, K_1, K_2, K_3 and P_1 and P_2 were employed.

b) A self-calibration was then carried out with only c, x_p, y_p and K_1 as APs.
c) The Z-D calibration parameters were determined as per Eqns. 2, 4 and 5 from the self-calibrations in (b) at three zoom settings only, namely zoomed fully out, mid zoom and zoomed fully in.
d) The empirically derived Z-D calibration parameters were then computed for the remaining two zoom settings (remaining three in the case of the PowerShot S30) and standard bundle adjustments were performed for these networks. The focus of the accuracy assessment was upon these surveys since the image correction procedure via the Z-D approach was fully independent of the corresponding self-calibration results.
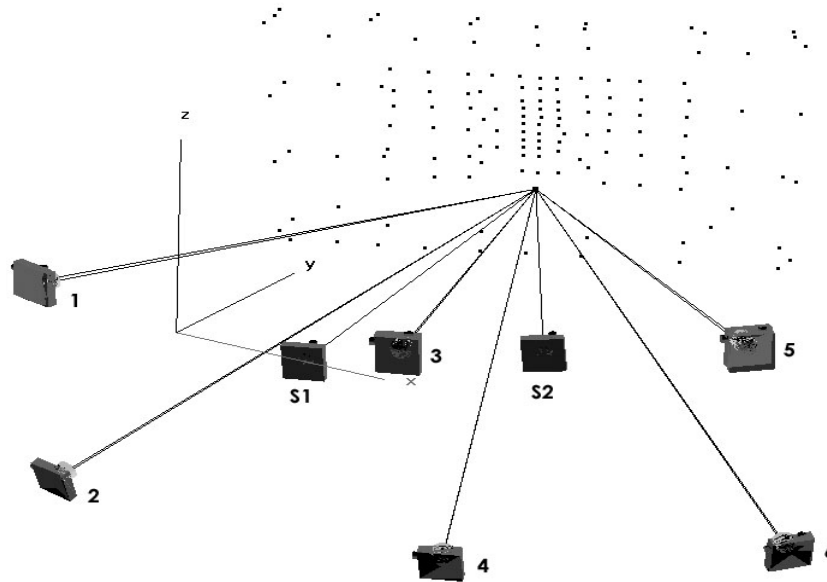
Figure 5. Target array and camera station geometry for the self-calibration networks.

RESULTS

Single Zoom Settings

Shown in Tables 2 to 5 are summaries of results for the four cameras. Part (a) of each table summarizes the outcome of the bundle adjustment with four self-calibration parameters only (c, x_p, y_p and K_1) for each zoom setting. Part (b) lists the results obtained in applying Z-D calibration in the networks where the self-calibrated values were not employed in the empirical modeling process. The tables afford an assessment of the impact of Z-D calibration on internal and external accuracy. For internal accuracy, the triangulation misclosures (RMS of image coordinate residuals) can be compared for the Z-D calibration and the corresponding self-calibration, and a measure of the effect on object space coordinate determination of the Z-D calibration approach is provided by the discrepancy between the XYZ coordinates obtained in each approach, which is provided in Part (b) of each table. With regard to absolute accuracy, the last column of Parts (a) and (b) of the tables list perhaps the most important accuracy measure, the RMSE against the true coordinate values, along with the equivalent proportional accuracy.

It is interesting to highlight some aspects of the results of self calibration and Z-D calibrations:

All of the cameras used in this investigation were inexpensive consumer grade digital cameras except for the Nikon D100, yet they produced relatively high 3D positioning accuracy. Moreover, as can be expected, the poorest accuracy is at the shortest focal length and the best is generally at the largest zoom. At the longest zoom setting the accuracy in object space ranged from 1:25,000 to 1:40,000, whereas for the shortest zoom setting, accuracy ranged from 1:9,000 to 1:17,000. Surprisingly, the most consistently accurate camera for all zoom settings was that with lowest resolution, namely the 2-megapixel IXUS V.

The relatively high accuracy of point determination is mostly a function of the high precision of image measurement. The RMS value of image coordinate residuals in the self-calibrations ranged from 0.05 to 0.15 pixels, with the precision being enhanced with increasing zoom.

From the mid range to the long focal lengths, the discrepancy between the object space coordinates obtained in the self-calibration and those from the Z-D calibration method is small. The discrepancy is largest at the short focal lengths.

Table 2. Results of Z-D calibration applied to the Nikon D100 with 24-85mm lens.

a) Results of self-calibrations with the four APs of c, x_p, y_p and K_1. The shaded rows are zoom settings not used for empirically determining Z-D calibration parameters.

Focal length (mm)	Number of object points	RMS of xy image coordinate residuals (pixels)	Mean std. error of XYZ (mm)	Diameter of object (mm)	RMSE against 'true' XYZ coords. in mm (proportional accuracy, 1:xx,000)
24	126	0.11	0.11	5070	0.54 (9)
35	110	0.10	0.07	3920	0.33 (12)
50	83	0.07	0.04	2780	0.24 (12)
70	60	0.07	0.03	2020	0.07 (28)
85	55	0.07	0.02	1490	0.06 (25)

b) Results of applying the Z-D calibration correction within the bundle adjustment.

Focal length (mm)	RMS of xy image coordinate residuals (pixels)	Mean std. error of XYZ (mm)	RMSE of XYZ coords. against self-cal with 4 APs, (mm)	RMSE against 'true' XYZ coords. in mm (proportional accuracy, 1:xx,000)
35	0.10	0.07	0.08	0.33 (12)
70	0.07	0.02	0.02	0.07 (28)

Table 3. Results of Z-D calibration applied to the Canon PowerShot G1.

a) Results of self-calibrations with APs of c, x_p, y_p and K_1. The shaded rows are zoom settings not used for empirically determining Z-D calibration parameters.

Focal length (mm)	Number of object points	RMS of xy image coordinate residuals (pixels)	Mean std. error of XYZ (mm)	Diameter of object (mm)	RMSE against 'true' XYZ coords. in mm (proportional accuracy, 1:xx,000)
7	135	0.15	0.22	5070	0.52 (10)
10.8	114	0.12	0.13	4480	0.37 (12)
16.8	81	0.06	0.03	2770	0.12 (23)
18.8	74	0.05	0.03	2450	0.12 (23)
21	65	0.06	0.03	2450	0.09 (27)

b) Results of applying the Z-D calibration correction within the bundle adjustment.

Focal length (mm)	RMS of xy image coordinate residuals (pixels)	Mean std. error of XYZ (mm)	RMSE of XYZ coords. against self-cal with 4 APs, (mm)	RMSE against 'true' XYZ coords. in mm (proportional accuracy, 1:xx,000)
10.8	0.22	0.26	0.64	0.59 (8)
18.8	0.08	0.05	0.13	0.14 (18)

Table 4. Results of Z-D calibration applied to the Canon IXUS V.

a) Results of self-calibrations with the four APs of c, x_p, y_p and K_1. The shaded rows are zoom settings not used for empirically determining Z-D calibration parameters.

Focal length (mm)	Number of object points	RMS of xy image coordinate residuals (pixels)	Mean std. error of XYZ (mm)	Diameter of object (mm)	RMSE against 'true' XYZ coords. in mm (proportional accuracy, 1:xx,000)
5.4	139	0.08	0.15	5070	0.30 (17)
6.7	134	0.07	0.12	4980	0.27 (18)
8.0	127	0.07	0.10	4570	0.22 (21)
9.3	112	0.06	0.08	3620	0.15 (24)
10.8	110	0.05	0.06	3750	0.12 (31)

b) Results of applying the Z-D calibration correction within the bundle adjustment.

Focal length (mm)	RMS of xy image coordinate residuals (pixels)	Mean std. error of XYZ (mm)	RMSE of XYZ coords. against self-cal with 4 APs, (mm)	RMSE against 'true' XYZ coords. in mm (proportional accuracy, 1:xx,000)
6.7	0.09	0.15	0.30	0.27 (18)
9.3	0.06	0.08	0.08	0.13 (28)

Table 5. Results of Z-D calibration applied to the Canon PowerShot S30.

a) Results of self-calibrations with the four APs of c, x_p, y_p and K_1. The shaded rows are zoom settings not used for empirically determining Z-D calibration parameters.

Focal length (mm)	Number of object points	RMS of xy image coordinate residuals (pixels)	Mean std. error of XYZ (mm)	Diameter of object (mm)	RMSE against 'true' XYZ coords. in mm (proportional accuracy, 1:xx,000)
7.1	138	0.11	0.13	5070	0.41 (12)
8.6	131	0.07	0.08	5070	0.18 (28)
10.3	115	0.07	0.06	4430	0.12 (37)
12.3	100	0.06	0.04	3920	0.08 (49)
17.5	74	0.05	0.03	2450	0.08 (31)
21.3	64	0.05	0.02	2020	0.05 (40)

b) Results of applying the Z-D calibration correction within the bundle adjustment.

Focal length (mm)	RMS of xy image coordinate residuals (pixels)	Mean std. error of XYZ (mm)	RMSE of XYZ coords. against self-cal with 4 APs, (mm)	RMSE against 'true' XYZ coords. In mm (proportional accuracy, 1:xx,000)
8.6	0.09	0.10	0.24	0.33 (15)
10.3	0.08	0.06	0.10	0.14 (32)
17.5	0.06	0.03	0.05	0.07 (35)

Mixed Zoom Settings

One of the main goals of Z-D calibration is to facilitate photogrammetric networks in which images can be recorded at whatever zoom settings suit the situation. As a final test of the Z-D calibration method, the technique was applied to three different network configurations of PowerShot S30 images, these being:

1) A 6-station network with two images each from zoom focal lengths of 8.6, 10.3 and 17.5mm. The stations occupied (approximately) the positions 1, 2, S1, S2, 5 and 6 in Fig. 5.
2) A 4-station geometry with two images each from 8.6 and 10.3mm focal lengths, the stations corresponding to positions 1, 2, 5 and 6 in Fig. 5.

3) A 2-station, nominally stereo configuration at a zoom focal length of 17.5mm, with the positions being at S1 and S2 in Fig. 5.

Shown in Table 6 for all three networks are the results of the bundle adjustments which utilized the empirically modeled Z-D calibration parameters. When it is recalled that the images from the three chosen zoom settings played no role in the determination of Z-D calibration parameters, the results are quite impressive. In all cases the absolute accuracy attained, while being less than that listed for the 12-station networks in Table 5, exceeded 1:15,000, even for the stereo case. Moreover, the triangulation misclosure values corresponded well to those from the self-calibration adjustments, being better than 0.1 pixel in all three networks. These results highlight the potential of the Z-D calibration method for networks incorporating images from different zoom settings.

Table 6. Empirical calibration model applied to different focal setting combinations for the PowerShot S30.

Focal lengths (mm)	RMS of xy residuals (pixels)	Mean std. error of XYZ (mm)	RMSE against 'true' XYZ coords. in mm (proportional accuracy, 1:xx,000)
2each @ 8.6, 10.3 & 17.5 = 6	0.07	0.26	0.32 (16)
2@8.6+2@10.3 = 4	0.07	0.27	0.33 (15)
2@17.5	0.02	0.07	0.11 (17)

CONCLUSIONS

The Z-D calibration approach has been shown to be viable for medium accuracy close-range photogrammetric applications involving consumer grade digital cameras. The method produces a 3D object point positioning accuracy well beyond that usually associated with such cameras, and certainly beyond the demands of many users of close-range photogrammetry. The Z-D calibration process is quite straightforward to implement, especially if one has the capability of fully automatic camera calibration, as exemplified by the *iWitness* system (Fraser & Hanley, 2004, Photometrix, 2006). *iWitness* employs colour coded targets and automatic camera identification to provide a virtually scale independent on-site camera self-calibration in a matter of minutes, with no prior knowledge of the camera being required. The real benefit of the Z-D calibration method is that it is very practical; once the image coordinate correction parameters are established, and there are supporting data processing facilities, the user of close-range photogrammetry is freed from the restrictions of recording images at fixed zoom/focus settings. This can greatly enhance the flexibility of moderate accuracy close-range photogrammetric measurement.

REFERENCES

Brown, D.C. (1966). Decentering distortion of lenses. *Photogrammetric Engineering*, 33(3): 444-463.
Brown, D.C. (1971). Close-range camera calibration. *Photogrammetric Engineering*, 37(8): 855-866.
Burner, A.W. (1995). Zoom lens calibration for wind tunnel measurements. *Videometrics IV*, Philadelphia, SPIE Vol. 2598: 19-33.
Fraser, C.S. (1980). Multiple focal setting self-calibration of close-range metric cameras. *Photogrammetric Engineering and Remote Sensing,* 46(9): 1161-1171.
Fraser, C.S. (1997). Digital camera self-calibration. *ISPRS International Journal of Photogrammetry & Remote Sensing*, 52: 149-159.
Al-Ajlouni, S. and Fraser, C.S. (2006). Zoom-Dependent Camera Calibration in Digital Close-Range Photogrammetry. *Photogrammetric Engineering and Remote Sensing,* (in Press).
Fraser, C.S. and Edmundson, K.L. (2000). Design and implementation of a computational processing system for off-line digital close-range photogrammetry. *ISPRS Int. Journal of Photogrammetry & Remote Sensing,* 55(2): 94-104.
Fraser, C.S and Hanley, H.B. (2004). Developments in close-range photogrammetry for 3D modelling: the *iWitness* example. Presented paper, International Workshop: *Processing and Visualization using High-Resolution Imagery,* Pitsanulok, Thailand, 18-20 November, 4 pages (on CD-ROM).

Fraser, C.S. and Shortis, M.R. (1990). A correction model for variation of distortion within the photographic field. *In: A. Gruen/ M. Baltsavias (Eds.): Close Range Photogrammetry Meets Machine Vision*, SPIE Vol. 1395: 244-251.

Fryer, J.G. (1986). Distortion in Zoom Lenses. *Australian Journal of Geodesy, Photogrammetry and Surveying*, 44: 49-59.

Fryer, J.G. and Brown, D.C. (1986). Lens distortion for close-range photogrammetry. *Photogrammetric Engineering and Remote Sensing,* 52(1): 51-58.

Laebe, T. and Foerstner, W. (2004). Geometric stability of low-cost digital consumer cameras. *International Archives of Photogrammetry, Remote Sensing & Spatial Information Sciences*, Vol. XXXV, Part B1: 528-534.

Noma, T., Otani, H., Ito, T., Yamada, M. and Kochi, N. (2002). New system of digital camera calibration. *International Archives of Photogrammetry, Remote Sensing & Spatial Information Sciences*, Vol. XXXIV, Part 5: 54-59.

Photometrix (2006). Website for *iWitness & Australis* systems, www.photometrix.com.au, accessed 2 Feb. 2006.

Wiley, A.G. and Wong, K.W. (1995). Geometric calibration of zoom lenses for computer vision metrology. *Photogrammetric Engineering & Remote Sensing*, 61(1): 69-74.